Low Profile Dual Band Dual Element MIMO Antenna for Sub-6 GHz 5G Applications

Kranti Patil
Dept. of Electronics and Telecommunication
G H Raisoni College of Engineering and Management, Pune, India
Dept. of Electronics and Telecommunication
Trinity Academy of Engineering, Pune, India

Mr. Dinkar Yadav
(Univ of Pune, SND College of
Engineering & Research Center, Yeola)

Abstract- **Here the design of two elements super compact antenna is explained for 5G band applications. The structure is analyzed with simulation and fabrication. Then after the results are compared. It found that almost similar parameters are achieved. Furthermore, it explains Performance Comparison in relation to prior work done in Literatures. A hexagonal ring for multiple input multiple output (MIMO) operating at Sub-6 GHz and suitable for wireless local area network (WLAN) applications for mobile devices is examined. The two antenna elements are built on a FR-4 substrate measuring 43 x 20 mm with a thickness of 0.8 mm. They are powered by two co-planar waveguide (CPW) fed techniques, enabling smooth operation with frequency spans of 3.24 - 3.62 GHz and 4.20 - 6.52 GHz, meeting the Sub-6 GHz and WLAN bands' bandwidth requirements. The two CPW grounds are linked together in order for it to be a viable option for MIMO practical applications. An Inverted-T-shaped radiator is also inserted between two ground planes, functioning as a decoupling structure to lesser interference between antenna parts. Furthermore, at two resonant frequencies of 3.5 and 4.9 GHz, respectively, the suggested MIMO antenna generates bandwidth of 11% in lower Sub-6 GHz and 43% in upper WLAN frequency bands, isolation >20dB, gain around 2.5dBi, and efficiency of 80% throughout the required bands. Ultimately, in Sub-6 GHz and WLAN operating bands, MIMO metrics such as envelope correlation coefficient (ECC) < 0.01 and diversity gain (DG) ~ 10dB are also attained. Manufactured antenna results are compared with simulated results. It finds almost equal parameters.**

Keywords: Sub-6 GHz, WLAN, hexagon ring low profile

I. INTRODUCTION

Currently, the merging of 5G and WLAN frequency bands into a single antenna that can be used to create MIMO configurations is garnering a lot of interest with the goal of implementing virtual communication. Greater dependability and data rate without the need for extra power and bandwidth are needed for virtual communication. The use of MIMO technology can help achieve this. As a result, MIMO technology with multiband operation is crucial. Numerous two-port MIMO antennas with various design approaches are documented in the literature that is currently in [1-10]. Reducing interference between antenna parts is the hardest part of constructing a MIMO antenna. Thus, MIMO antennas with various decoupling structure designs are also documented in the literature.

The method of simulation and fabrication of a dual-port antenna system for cognitive radio (CR) applications is explained in [1]. The isolation and envelope correlation coefficient (ECC) are measured to be greater than 18 dB and less than 0.12, respectively. An integrated decoupling technique is described in various articles, which increases the adaptability of multiport, multiband antenna designs and streamlines the antenna structure. [2] In this case, the isolation level was greater than 20 dB and the ECC was less than 0.04. Article [3] examined about various methods for attaining isolation in a MIMO antenna design.

In [4], the development of a triple band Microstrip patch antenna as a defective ground plane is described. It is based on modified split ring resonators (SRR) and modified complementary split ring resonators (CSRR). The 35 mm x 35 mm × 1.6 mm FR4 substrate with a dielectric constant of 4.4. A robust, uncomplicated, and lightweight ultra-wideband (UWB) bowl-shaped monopole antenna is suggested in [5] and utilized to construct a 3 × 3 multiple input multiple output (MIMO) antenna.

An ultra-wide band of 2.3–8.1 GHz (5.8 GHz, 111.5%) and a strong isolation of more than 20 dB

between the antenna elements of the MIMO antenna may be achieved in this case, according to the simulated and observed results. Article [6] proposes a miniaturized increased isolation 8-unit MIMO antenna for cellphones. Here, they were able to obtain more than 25 dB of isolation, less than 0.08 envelope correlation coefficient, more than 50% radiation efficiency, and gain between 4.2 and 5.3 dBi across the complete working frequency range for the suggested MIMO antenna. In [7] For WLAN applications, an isolation enhancement for a closely spaced quad port multiple-input multiple-output (MIMO) antenna is provided. It is possible to attain MIMO parameters such as an envelope correlation coefficient (E.C.C.) of less than 0.5 and a diversity gain (D.G.) of 10 dB. In [8], fifth-generation (5G) terminal applications, an 8 × 8 MIMO antenna system with multiple decoupling structures is suggested in this article. Initially, an antenna element is presented, which consists of two Bent-L shaped monopoles with dimensions of 12.7 × 6.1 mm2 and an L-shaped open slot of 5.6 × 5 mm2. Each antenna element's overall efficiency has increased from a worst 20% to over 45%, and the average isolation has been optimized from 13.2 dB to 21.9 dB. Additionally, for the targeted frequency bands, the computed envelop correlation coefficient (ECC) is less than 0.01 and the mean efficiency gain is less than 1 dB.

New developments in reconfigurable technology for wireless communication systems offer a range of international solutions. A quad port multipolar zed switchable multiple input multiple output (MIMO) antenna for sub-6 GHz applications is presented [9] in this research paper. [10] Trial and error techniques are usually used in the construction of massive multiple-input multiple-output (m-MIMO) antennas. The goal of this research is to identify a practical optimization technique for more effective antenna is explained. A planar dual-band multiple-input multiple-output (MIMO) antenna design for the potential fifth-generation (5G) frequency bands of 28 and 38 GHz is shown in this paper [11]. For 5G wireless communication, a palm tree-shaped high-isolation wideband MIMO (Multiple-Input Multiple-Output) antenna is being developed. The proposed MIMO antenna is designed with a FR4 substrate [12]. A tiny dual band notched ultra wide band (UWB) multiple input multiple output (MIMO) antenna is suggested in [13]. The suggested MIMO UWB antenna includes two slotted rectangular radiating structures, a Microstrip feed line, and a slotted. The design, analysis, and experimental validation of a small 2x1 MIMO antenna that operates in two bands are presented in this study [14]. Fifth Generation (5G) uses frequency 1, which is Linearly Polarized (LP) with Spatial Diversity running in the sub-6 GHz frequency. Band. In [15] Two suggested multiple input multiple output antenna elements (MIMOs) with good performance in the 5G spectrum are designed, fabricated, measured, and reported in this study.

It is clear from the aforementioned antennas [1–15] that there is a significant market for MIMO antennas that support mobile devices in the sub-6 GHz 5G and WLAN bands. Thus, for wireless applications in mobile devices, this study presents the design and analysis of a two-port MIMO antenna with a hexagonal ring shape that operates in both the WLAN and 5G sub-6GHz bands.

II. Single Proposed Hexagonal Ring Shaped Geometry and Design

Figure 1 shows the planned hexagonal ring-shaped antenna's designed geometry, structure, and precise dimensions.

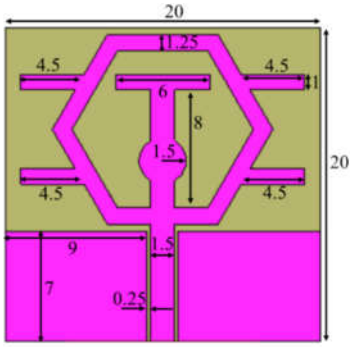

Figure 1 Structural layout of proposed hexagonal ring shaped antenna (dimensions are measured in mm)

Figure 1 shows that the front side of the FR-4 substrate has an embossed 50Ω transmission line with an area of 7.5×1.5mm2 and a CPW ground plane. The thickness (h), dielectric permittivity (ε_r), and loss tangent (tanδ) of the substrate are 0.8mm, 4.3, and 0.025, respectively. The antenna is a hexagon-shaped ring that is positioned just above the feed line, with an outside

radius of 7 mm and an inner radius of 5.75 mm. Additionally, a radiator in the form of a tap is etched between the structures of hexagonal rings. The tap-shaped radiator is made up of a T-shaped strip with a 1.5 mm-radius circular strip designed in the middle of the vertical T-shaped strip. The horizontal strip in a T-shaped radiator measures 6×1 mm2, whereas the vertical strip measures 6*1mm2. Lastly, four horizontal strips, each measuring 4.5 x 1 mm2, are put into the hexagon-shaped ring's center diagonal. The entire structure, with a 20 x 20 mm2 planned footprint, aids in getting the WLAN band and the intended sub-6 GHz frequency for use in mobile devices.

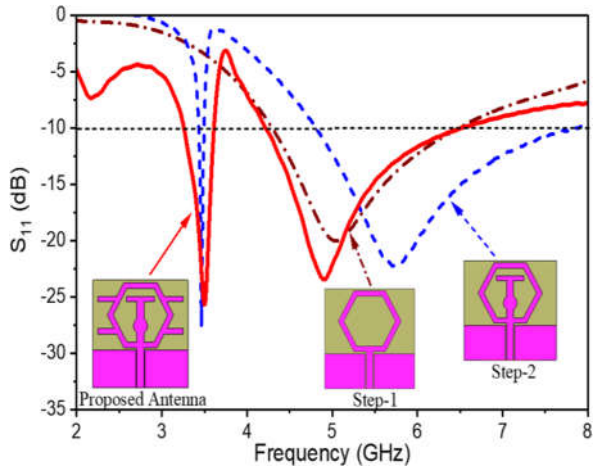

Figure 2 Stepwise design along with S_{11} (dB) of proposed hexagonal ring shaped antenna

Figure 2 shows the step-wise designed together with the S11 parameter to help visualize the developed structure of the suggested hexagonal ring shaped antenna. Figure 2 (Step-1) illustrates how the CPW fed approach first excites a hexagon ring. This time, Step-1 is able to produce the resonance at 5 GHz with an S11 magnitude of -20dB and a frequency range of 4.31-6.48 GHz. This validates that the hexagonal ring-shaped structure and the CPW-fed have the correct impedance matching. Furthermore, in Step 2, a tap-shaped radiator protrudes from the hexagonal ring's bottom edge, creating a frequency band between 3.43 and 3.49 GHz. This creates a higher frequency band with a range of 4.82 to 7.80 GHz, with respective center frequencies of 3.46 and 5.75 GHz. It also shifts the previously generated frequency band to the higher side. Lastly, Step-3 is constructed as shown in Figure 2 to increase the bandwidth of 3.43 - 3.49 GHz and to move the resonance of 5.75 GHz to the lower side. Two resonances at 3.5 GHz and 4.9 GHz can be produced by the Step-3 using frequency bands that span 3.24 - 3.62 GHz and 4.20 - 6.51 GHz, respectively.

Figure 3 shows the surface current distribution analysis at two resonance frequencies of 3.5 GHz and 4.9 GHz, which further validates the step-wise design method. The tap-shaped radiator and the lower portion of the hexagonal ring are seeing increased current flow at 3.5 GHz, as shown in Figure 3(a), which helps to generate the lower (3.24 - 3.62 GHz) frequency bands. The hexagonal ring in Figure 3(b) at 4.9 GHz is where the largest current is observed to be flowing, confirming its role in the creation of upper (4.20 - 6.52 GHz) frequency bands. Thus, it can be concluded from the examination of the surface current distribution and step-by-step design mechanism that the suggested hexagonal ring antenna is a strong candidate for WLAN and Sub-6 GHz applications for mobile devices.

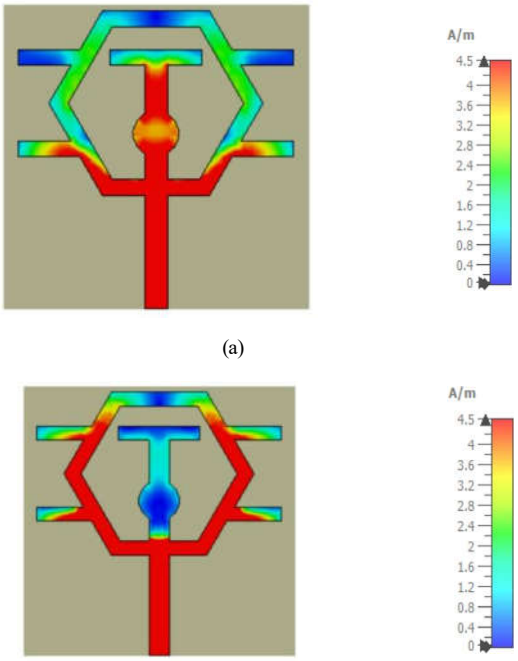

Figure 3 Surface current distribution of proposed hexagonal ring shaped antenna (a) at 3.5 GHz (b) at 4.9 GHz

III. GEOMETRY LAYOUT OF TWO-PORT HEXAGONAL RING SHAPED MIMO ANTENNA

Figure 4 shows the suggested hexagonal ring-shaped two-port MIMO antenna's geometric arrangement and design, which includes an inverted T-shaped isolating element. The two antenna elements that are suggested are built on a FR-4 substrate with dimensions of 43x20 mm2, a dielectric constant of 4.3, and a loss tangent of 0.02. To accommodate a larger number of antennas with small sizes, the spacing between the edges of two antenna elements is reserved at 3 mm. As shown in Figure 4, an Inverted-T shaped isolating device is inserted between the antennas to lessen interference between the elements. For the purpose of analyzing the features of transmission coefficient and impedance matching, the entire MIMO antenna construction is taken into consideration.

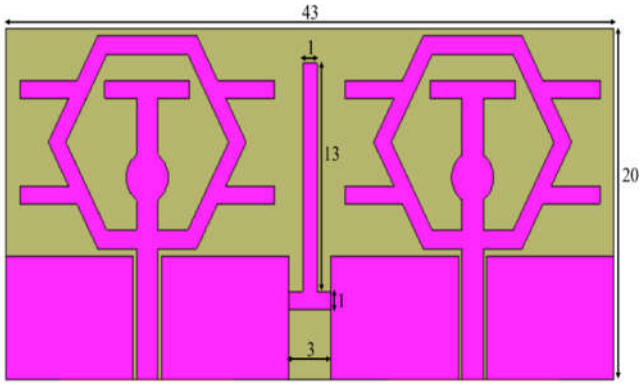

Figure 4 Geometry layout of proposed Two Port hexagonal ring shaped MIMO antenna

IV. RESULTS AND DISCUSSION OF PROPOSED TWO-PORT HEXAGONAL RING SHAPED MIMO

CST MWS software is used to assess the proposed two-port MIMO antenna with a hexagonal ring form. The validation of the design takes into account many characteristics, such as the reflection coefficient (S11) dB, transmission coefficient (S12) dB, gain, efficiency, ECC, and DG, as well as the surface current (A/m) distribution.

A. S_{11} (dB) and S_{12} (dB) versus Frequency (GHz) Characteristics:

Figure 5 shows the S-characteristics, which include S11 (dB)/S22(dB) and S12 (dB)/S21(dB). It is evident from the S11 and S22 curves that two resonances at 3.5 GHz and 4.9 GHz validate that the two-port MIMO antenna can operate with ease in the frequency range of 3.24 - 3.62 GHz and 4.20 - 6.51 GHz, respectively, satisfying the Sub-6 GHz and WLAN frequency bands' impedance bandwidth requirements for mobile device applications. The correct impedance matching in the intended operating bands is ensured by the precise matching of the S11 and S22 curves. In the lower Sub-6 GHz and upper WLAN frequency bands, the achieved -10 dB impedance bandwidth is 11% and 43%, respectively. Moreover, it is seen that the S12/S21 curves (shown by dotted and dashed blue lines, respectively) guarantee a minimum isolation of greater than -20 dB in the upper WLAN and lower Sub-6 GHz frequency bands. This confirms that, when operating simultaneously in lower Sub-6 GHz and upper WLAN frequency bands, the two antenna elements are properly isolated from one another thanks to the Inverted-T shaped isolating structure while keeping the compactness and stay shielded from each other's interference.

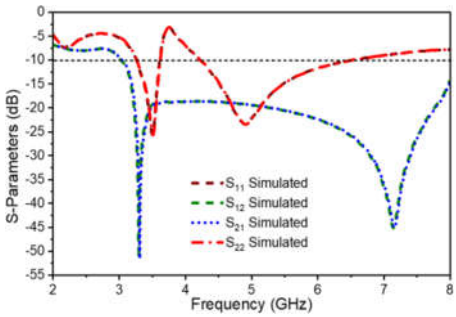

Figure 5 S-characteristics of proposed hexagonal ring shaped two-port MIMO antenna

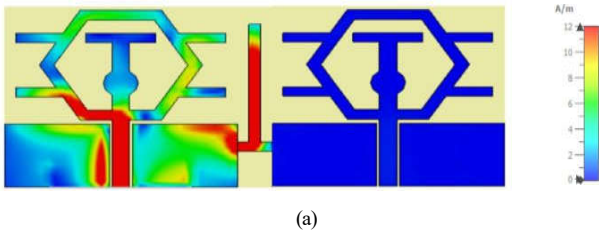

(a)

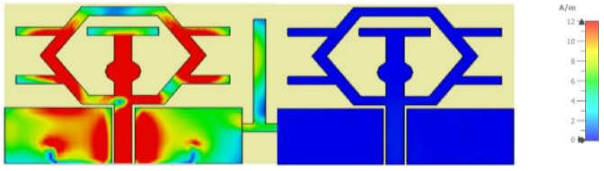

(b)

Figure 6 Surface current dsitribution of proposed hexagonal ring shaped two-port MIMO antenna (a) at 3.5 GHz and (b) at 4.9 GHz

B. Gain (dBi) and Efficiency (%) Versus Frequency (GHz) characteristic:

Figure 7 shows the characteristics of the proposed hexagonal ring-shaped two-port MIMO antenna in terms of gain (dBi) and efficiency (%) vs frequency (GHz). Due to brevity, Figure 7 only shows the gain and efficiency of one antenna element while Figure 6 shows the mirror image far-field radiation patterns for both antenna elements. Figure 7 shows that for mobile device applications, the MIMO antenna offers gain greater than 2dBi and radiation efficiency ranging from 80 to 90% in both the lower Sub-6 GHz and upper WLAN frequency bands.

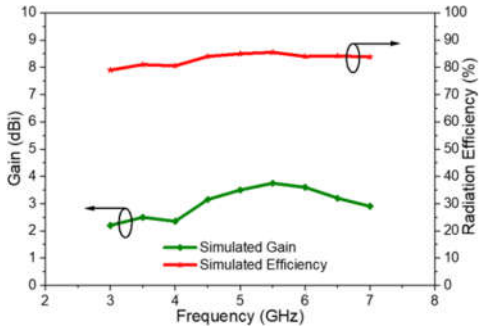

Figure 7 Gain and efficiency of Proposed hexagonal ring-shaped two-port MIMO

C. Envelope Correlation Coefficiency (ECC) Versus Frequency (GHz) characterisitc:

The simulated ECC versus frequency (GHz) characteristic of the suggested two-port MIMO antenna with a hexagonal ring shape is shown in Figure 8 for the intended operating bands. In order to analyze the correlation between two antenna elements, the ECC values are simulated from S-parameters and radiation patterns. The ECC values from S-parameters and far field patterns are confirmed to be less than 0.01 across the operating band of operation by looking at Figure 8. This attests to the two antenna elements' good separation from one another and their capacity to produce uncorrelated signals in the intended operating bands.

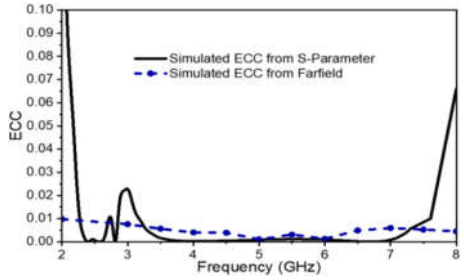

Figure 8 ECC of Proposed hexagonal ring-shaped two-port MIMO antenna

D. Diversity Gain (DG) (dB) versus Frequency (GHz) characteristic:

The suggested hexagonal ring-shaped two-port MIMO antenna's simulated DG (dB) against frequency (GHz) characteristic is shown in Figure 9. Throughout the working band of operation, it is evident that DG values are substantially closer to 10 dB based on both the S-parameters and far field radiation patterns.

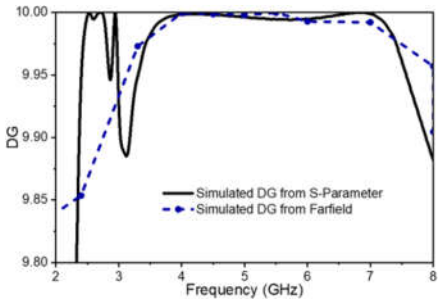

Figure 9 DG values of proposed hexagonal ring shaped two-port MIMO

V. MEASURED RESULTS OF FABRICATED ANTENNA

The simulated antenna presented in this study was manufactured using the MITS-Eleven Lab printed circuit board machine, with a FR 4 substrate. It consists of two antenna elements positioned on a compact substrate measuring on 43 mm^2 × 20 mm^2, as depicted in Figure 10. The substrate was 0.8 mm thick. To verify the accuracy of the simulated results, measurements were conducted on an Agilent N5230A vector network analyzer (VNA).

(a) (b) (c)

Figure 10: Fabricate Antenna a) prototype b) Antenna with BNC connector c) Measurement setup with VNA

Furthermore, radiation characteristics were evaluated within an anechoic chamber. The measured results are compared with the simulation results to validate the

antenna's performance. Figure 11 displays the S-parameter results, presenting a comparison between measured and simulated data. The analysis reveals that the values for S12 were consistently below − 27 dB across the entire frequency band range. These findings suggest that the proposed prototype exhibits minimal interference or coupling between its ports.

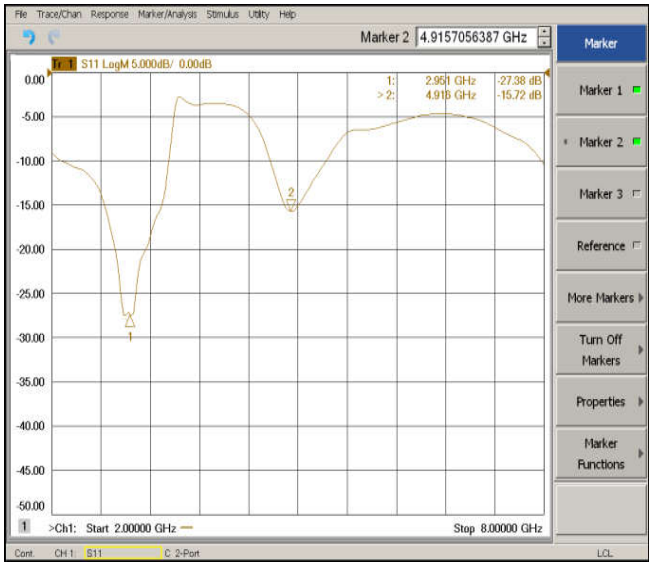

Figure 10: Fabricated Antenna – S11 parameter

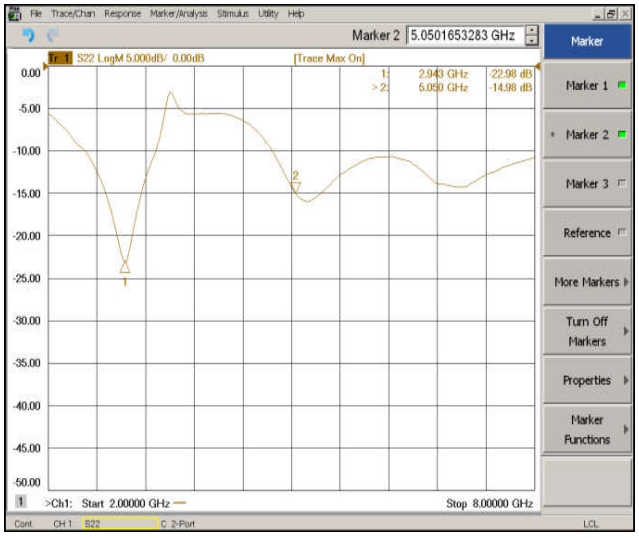

Figure 11: Fabricated Antenna – S22 parameter

From Figure 10 and 11, it can be seen that S11 & S22 parameters at frequency 5.00 Ghz are almost same value which is 25 dB. This indicates that the perfect impedance matching has achieved. This is the good indication for validation of manufactured antenna in expected application of 5G band.

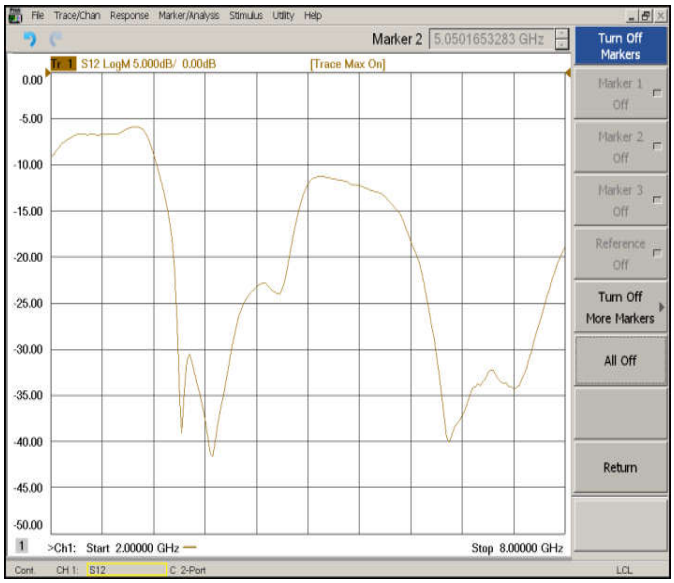

Figure 12: Fabricated Antenna – S12 parameter

From Figure 12 and 13, it is clearly seen that S21 and S12 parameters are perfectly matched at frequency 5Ghz.

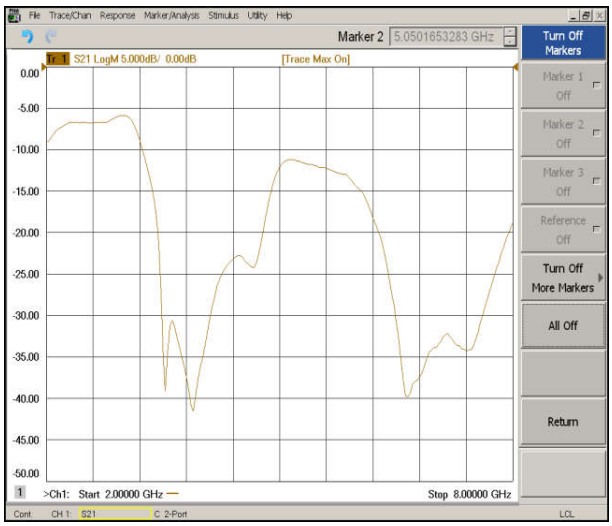

Figure 13: Fabricated Antenna – S21 parameter

High isolation between antenna elements is very essential in MIMO antenna. Isolation techniques helps to reduce mutual coupling and enhance overall performance. Maintaining an optimal VSWR is crucial for efficient antenna operation specifically in 5G

services. Here with this fabricated antenna, VSWR value comes up to unity at resonance frequency.

From figure 14 it is clear that voltage standing wave ratio is having unity value at the resonance frequency at 3.5 Ghz.

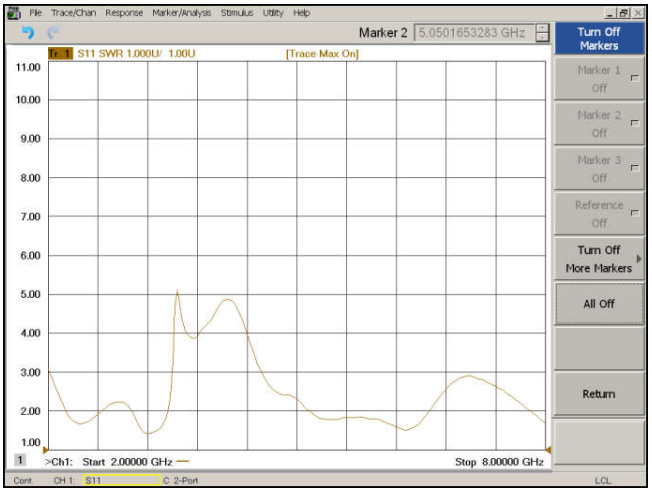

Figure 13: Fabricated Antenna –VSWR parameter

Table 1 explains the sample VSWR values (Real) for different frequencies. It comes nearly to 0.1

Table 1 Sampeled SWR data for diff frequency

Freq(Hz)	S11(REAL)	S12(REAL)	S21(REAL)	S22(REAL)
2000000000	0.0745439	-0.31947824	-0.3191755	0.0008957
2030000000	0.1145172	-0.31404769	-0.3138386	0.0350272
2060000000	0.1499839	-0.30980402	-0.3099127	0.0740568
2090000000	0.1794812	-0.29427117	-0.2940526	0.1043701
2120000000	0.2024426	-0.27208644	-0.272101	0.1220304
2150000000	0.2207377	-0.23475969	-0.2347882	0.1269789
2180000000	0.2275272	-0.19112085	-0.1910572	0.1357783
2210000000	0.2244449	-0.14188401	-0.1415584	0.1428639

The formula to measure the gain is,

$G_{AUT} = (P_{R2}/P_{R3}) * G_{Ref}$ ..... (i)

G_{AUT} = Gain of Antenna Under Test

P_{R2} = Power Recived by Refence Antenna

P_{R3}= Power Recived by Antenna Under Test

G_{Ref} = Gain of Reference Antenna

For Gain calculation we can use the above formula, Initially P_{R2} (Radiated Power) and P_{R3} (Gain Power) can be calculated. These parameters are measured in dBm. While doing this it is needed to convert dBm into dB {as (dBm –30) = dB}. Then as per respective frequency in table shown below we have to select the reference gain as shown in figure 14. Once we get reference gain, we can find out gain of designed antenna (G_{AUT}) in dBi.

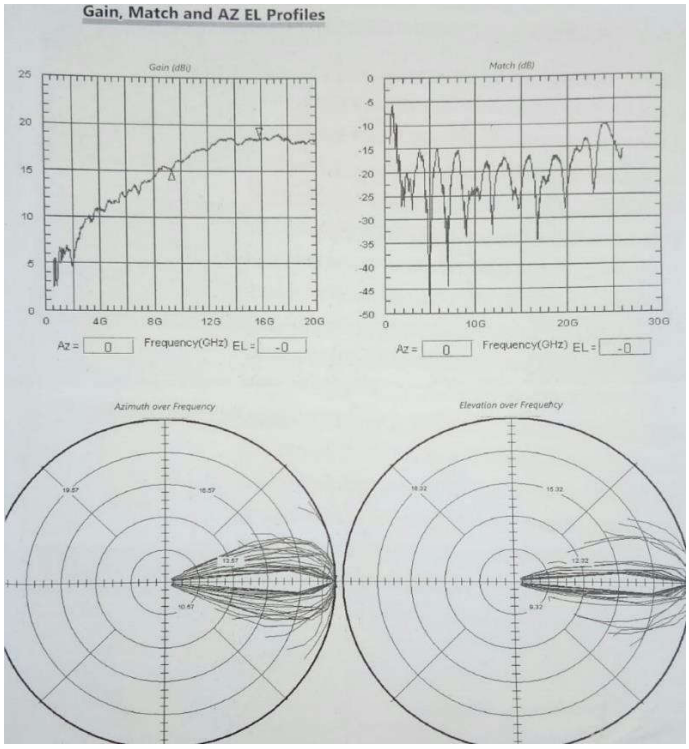

Figure 14 : Gain of reference antenna (G_{Ref})

The detailed Comparison of this simulated antenna with previous simulated designs are mention in table given below. Table 1 explains Performance Comparison in relation to prior work done in Literature.

Table 1 Performance comparision in relation to prior work done in Liturature

Ref.	No of Elements	Size(mm^3)	Substrate	Operating Frequency(Ghz)	Gain (dBi)	Isolation(dB)	Isolation Technique	Applications
[15]	4	25*12*0.3	Roger RT/Duroid 5880	1.8 -2.6	7.2	≥17	Tapered slot	Integrated 5 G/4 G in the same structure, mm-wave
[16]	4	30.5*2*0.5	FR4	25-40	6.1	≥9.7		5 G applications
[17]	2	48*35*1.6	FR4- epoxy	3.2- 4.2	2.8	≥20	Metamaterials (SRR)	UWB applications
[18]	4	60*60*1.6	FR4	2.1-18	10.55	≥17.5	EGB	Modern wireless communication systems
[19]	2	50*30*1.6	FR4	3- 16.2	7.4	≥20	F-shaped stubs	UWB applications
[20]	4	80*80*1.6	FR4	2.5- 14.5	5.8	≥25	H- and U-slots	WiMAX and military/radar applications
[21]	4	48*52*1.6	FR4	2.1-20	3.5	≥20	Asymmetric coplanar strip (ACS) feed	WLAN applications
[22]	4	18*16*1.57	RT/Duroid 5870	2.7- 11	7.98	≥24	DNG metamaterial superstrate	5 G communications
[23]	4	36*36*5	Rogers RT 4003	5.6- 6.05	10	≥25	FSS	low profile smart devices at mm-wave 5 G applications
[24]	4	24*20*1.5	Transparent conductive sheet AgHT-8	36.6- 39.5	3	≥16	Undivided ground plane	5G mm-wave applications
[25]	4	80*80*1.5	Rogers 5880	24.10 -27.18	12	≥20		5G mm-wave applications
[26]	4	30*35*1.5	Rogers R04350B	33-44.13	8.3	≥10	Zig-zag shaped DGS Substrate integrated	Multichannel millimetre-wave transceivers

[27]	2		Rogers RT/Duroid 588	23-40	8.2	≥20	waveguide (SIW)	mm-wave applications
[28]	2*2	41*46*1.5	Rogers RT/Duroid 588	27.5- 31.44	13.1	≥23	U-slots	mm-wave applications
Proposed One	2	43*20*0.8	FR 4	3.24- 6.52	2.5	≥20	Inverted T Radiator	WLAN & Sub 6- Ghz

Conclusion

Effective analysis is done on the new hexagonal ring-shaped two-element array design for sub-6 GHz and WLAN frequency bands in mobile device applications. The suggested two-port MIMO antenna with a hexagonal ring shape is straightforward to construct, small in size, and can be put inside actual mobile devices to function in the intended operating bands. It is constructed on an affordable, readily accessible FR-4 substrate. Additionally, in the appropriate operating ranges needed for mobile device applications, it shows good impedance bandwidth, high isolation, radiation patterns, ECC, and DG properties. The fabricated device has almost similar results as simulated one. This shows good indication of validation in mobile devices for expected operating band application.

Reference

[1] R. K. Parida et al., "A Compact Isolated CR Antenna System for Application in C-Band," Int. J. Antennas Propag., vol. 2024, no. 1, 2024, doi: 10.1155/2024/5522356.

[2] S. Sengar, P. K. Malik, P. Chandra Srivastava, K. Srivastava, and A. Gehlot, "Performance Analysis of MIMO Antenna Design with High Isolation Techniques for 5 G Wireless Systems," Int. J. Antennas Propag., vol. 2023, 2023, doi: 10.1155/2023/1566430.

[3] E. Suganya, T. Prabhu, S. Palanisamy, P. K. Malik, N. Bilandi, and A. Gehlot, "An Isolation Improvement for Closely Spaced MIMO Antenna Using /4 Distance for WLAN Applications," Int. J. Antennas Propag., vol. 2023, 2023, doi: 10.1155/2023/4839134.

[4] D. Allin Joe and T. Krishnan, "A Triband Compact Antenna for Wireless Applications," Int. J. Antennas Propag., vol. 2023, 2023, doi: 10.1155/2023/5344999.

[5] C. Li, P. Wen, X. Lin, D. Wu, and C. Zhou, "An Ultra-Wideband MIMO Bowl-Shaped Monopole Antenna with Sturdy and Simple Construction," Int. J. Antennas Propag., vol. 2023, 2023, doi: 10.1155/2023/5667834.

[6] J. Guo, S. Zhang, C. Z. Han, and L. Zhang, "Combined Open-Slot and Monopole 8 × 8 High-Isolation Broadband MIMO Antenna System for Sub-6 GHz Terminals," Int. J. Antennas Propag., vol. 2023, 2023, doi: 10.1155/2023/5169206.

[7] R. Ma, H. Huang, X. Li, and X. Wang, "Triple-Band MIMO Antenna with Integrated Decoupling Technology," Int. J. Antennas Propag., vol. 2023, 2023, doi: 10.1155/2023/6691346.

[8] D. Thangarasu, S. K. Palaniswamy, and R. R. Thipparaju, "Quad Port Multipolarized Reconfigurable MIMO Antenna for Sub 6 GHz Applications," Int. J. Antennas Propag., vol. 2023, 2023, doi: 10.1155/2023/8882866.

[9] A. Biradar et al., "Massive MIMO Wireless Solutions in Backhaul for the 5G Networks," Wirel. Commun. Mob. Comput., vol. 2022, 2022, doi: 10.1155/2022/3813610.

[10] T. Upadhyaya et al., "Aperture-Fed Quad-Port Dual-Band Dielectric Resonator-MIMO Antenna for Sub-6 GHz 5G and WLAN Application," Int. J. Antennas Propag., vol. 2022, 2022, doi: 10.1155/2022/4136347.

[11] M. Kanagasabai, S. Shanmuganathan, M. G. N. Alsath, and S. K. Palaniswamy, "A Novel Low-Profile 5G MIMO Antenna for Vehicular Communication," Int. J. Antennas Propag., vol. 2022, 2022, doi: 10.1155/2022/9431221.

[12] T. Govindan, S. K. Palaniswamy, M. Kanagasabai, and S. Kumar, "Design and Analysis of UWB MIMO Antenna for Smart Fabric Communications," Int. J. Antennas Propag., vol. 2022, 2022, doi: 10.1155/2022/5307430.

[13] S. Basir, K. S. Alimgeer, S. A Ghauri, M. Maqsood, M. Sarfraz, and M. Y. Ali, "MIMO Antenna with Notches for UWB System (MANUS)," Int. J. Antennas Propag., vol. 2022, 2022, doi: 10.1155/2022/4870661.

[14] M. H. Almalki, A. Adnan, and A. Syed, "Design of Dual-Band , 4-Ports MIMO Antenna-Diplexer Based on Quarter-Mode Substrate Integrated Waveguide," vol. 2022, 2022.

[15] E. Al Abbas, M. Ikram, A. T. Mobashsher, and A. Abbosh, “MIMO antenna system for multi band millimeter-wave 5G and wideband 4G mobile communications,” IEEE Access, vol. 7, pp. 181916–181923, 2019.

[16] L. Chang and H. Wang, “Miniaturized wideband four-antenna module based on dual-mode PIFA for 5G 4 × 4 MIMO applications,” IEEE Transactions on Antennas and Propagation, vol. 69, no. 9, pp. 5297–5304, 2021.

[17] H. Sakli, C. Abdelhamid, C. Essid, and N. Sakli, “Metamaterial based antenna performance enhancement for MIMO system applications,” IEEE Access, vol. 9, pp. 38546–38556, 2021.

[18] W. Wu, B. Yuan, and A. Wu, “A quad-element UWB-MIMO antenna with band-notch and reduced mutual coupling based on EBG structures,” International Journal of Antennas and Propagation, vol. 2018, Article ID 8490740, 10 pages, 2018

[19] A. Iqbal, O. A. Saraereh, A. W. Ahmad, and S. Bashir, “‘Mutual coupling reduction using F-Shaped stubs in UWB-MIMO antenna,” IEEE Access, vol. 6, pp. 2755–2759, 2018.

[20] V. S. D. Rekha, P. Pardhasaradhi, B. T. P. Madhav, and Y. U. Devi, “Dual band notched orthogonal 4-element MIMO antenna with isolation for UWB applications,” IEEE Access, vol. 8, pp. 145871–145880, 2020.

[21] A. Ibrahim and W. Ali, “High isolation 4-element ACS-fed MIMO antenna with band notched feature for UWB communications,” International Journal of Microwave and Wireless Technologies, vol. 14, no. 1, pp. 54–64, 2022.

[22] R. Mark, N. Rajak, K. Mandal, and S. Das, “Metamaterial based superstrate towards the isolation and gain enhancement of MIMO antenna for WLAN application,” AEUInternational Journal of Electronics and Communications, vol. 100, pp. 144–152, 2019.

[23] A. A. Ibrahim, W. A. E. Ali, M. Alathbah, and A. R. Sabek, “Four-port 38 GHz MIMO antenna with high gain and isolation for 5G wireless networks,” Sensors, vol. 23, no. 7, p. 3557, 2023

[24] A. Desai, C. D. Bui, J. Patel, T. Upadhyaya, G. Byun, and T. K. Nguyen, “Compact wideband four element optically transparent MIMO antenna for mm-wave 5G applications,” IEEE Access, vol. 8, pp. 194206–194217, 2020.

[25] D. A. Sehrai, M. Abdullah, A. Altaf et al., “A novel high gain wideband MIMO antenna for 5G millimeter wave applications,” Electronics, vol. 9, no. 6, p. 1031, 2020.

[26] M. Khalid, S. Ifat Naqvi, N. Hussain et al., “4-Port MIMO antenna with defected ground structure for 5G millimeter wave applications,” Electronics, vol. 9, no. 1, p. 71, 2020.

[27] K. Patil, S. Botkar, J. Kulkarni and A. Desai, "Design of Hexagonal Ring Shaped Two Port MIMO Antenna for Sub-6 GHz and WLAN Application for Mobile Devices," *2022 IEEE Wireless Antenna and Microwave Symposium (WAMS)*, Rourkela, India, 2022, pp. 1-6, doi: 10.1109/WAMS54719.2022.9847934.

[28] B. Yang, Z. Yu, Y. Dong, J. Zhou, and W. Hong, “Compact tapered slot antenna array for 5G millimeter-wave massive MIMO systems,” IEEE Transactions on Antennas and Propagation, vol. 65, no. 12, pp. 6721–6727, 2017.

[29] N. Yoon and C. Seo, “A 28-GHz wideband 2×2 U-slot patch array antenna,” Journal of electromagnetic engineering and science, vol. 17, no. 3, pp. 133–137, 2017.

[30] Bhattacharya, A., Roy, B., De, A., Chakraborty, U., & Kumar Bhattacharjee, A. (Eds.). (2023). Advances in Microwave Engineering: From Novel Materials to Novel Microwave Applications (1st ed.). CRC Press. https://doi.org/10.1201/9781003459880